MAGNETIC ASSIST

Mohammadhossein Ezzati , Valeh School, mhe8795@gmail.com

ARTICLE INFO

IranTeam Member IYPT 2025 , Lund University, Sweden

Advisors: Alireza Noroozshad,

Mohammad Mahdi Shariatmadar

Accepted by Ariaian Young Innovative

Minds Institute , AYIMI

http://www.ayimi.org ,info@ayimi.org

ABSTRACT

Attach one or two magnets to a non-magnetic and non-conductive base such that they attract a magnet suspended from a string. The magnetic pendulum is a striking example of unpredictability in classical physics; a magnetic bob suspended above fixed magnets on a non-magnetic surface exhibits chaotic motion when released. In this study, we investigate the parameters affecting the motion of the moving magnet.

Keywords : *Magnetic Pendulum, Non-Magnetic Base, Non-Conductive Base, Chaotic Motion*

1. Introduction

The magnetic pendulum is a striking example of unpredictability in classical physics; a magnetic bob suspended above fixed magnets on a non-magnetic surface exhibits chaotic motion when released. In this study, we investigate the parameters affecting the motion of the moving magnet.

Guiding questions are intended as inspiration for beginning our project as :

- How is the magnetic pendulum influenced by the other magnets?
- What forces are at work?
- the instruction and arrangement the magnets should attract each other?
- An arrangement that "supports" the pendulum for example to increase the amplitude beyond the starting amplitude?

In a magnetic pendulum many small rotating magnetic dipoles (on the left,) can create an effective macroscopic field, (on the right). This effective field can exert a torque or lateral force on the moving magnet, leading to rotational or orbit-like motion, which is what we observe experimentally.

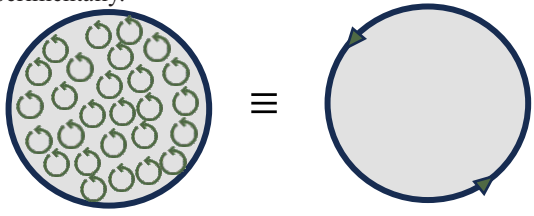

Fig.1: Magnetic dipoles and microscopic field

Three phases should be considered as :

Phase1. Perturbation Initiation

Phase2. Dynamic Oscillation

Phase3. Equilibrium Stabilization

Now suppose the pendulum consists of a magnet suspended from a string. The plane under the pendulum contains a distribution of like magnets which, based on their number and placement, should affect the dynamics of the pendulum.

Here again external forces are ;

Magnetic Force, Drag Force, Gravitational Force and String Tension Force (Fig. 2).

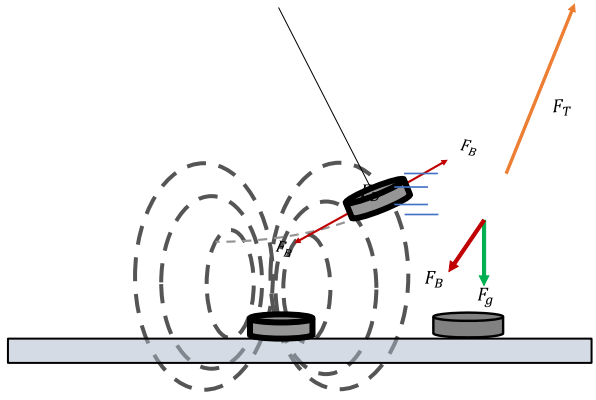

Fig.2: External Forces

2. Quantitative Analysis

In this setup, the magnetic field is generated by permanent magnets fixed on a non-magnetic base. The field depends on the shape, size, and orientation of the magnets, as well as their distance from the suspended magnet.

Magnetic Field:

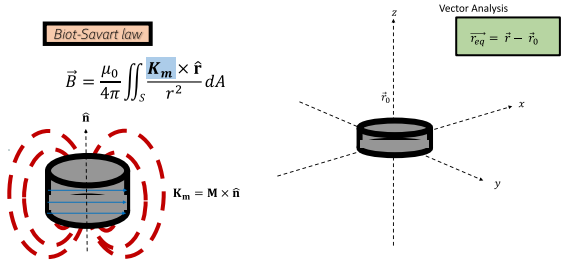

Fig.3: Magnetic Field

The source of the field is the internal magnetic structure of the materials, which creates a specific pattern in space. This field interacts with the suspended magnet and causes it to move, oscillate, or stabilize depending on its position and initial motion.

$\mathbf{m} = \iiint M\, dV$ Dipole Characterization

Dipole Magnet

$$\vec{B} = \frac{\mu_0}{4\pi}\frac{1}{r^3}[3(\vec{m}.\vec{r_{eq}})\hat{r} - \vec{m}]$$

Lorentz Force

$$\vec{F}_{mag} = \iint_S \vec{\mathbf{K}}_{\mathbf{m}}\, dS \times \vec{B}$$

The magnetic field of a dipole depends on its direction and the position of the observation point.

$$m_r = \mathbf{m}\,.\,\hat{\mathbf{r}} = m_x \sin\theta\cos\phi + m_y \sin\theta\sin\phi + m_z\cos\theta$$

$$B_r = \frac{\mu_0}{4\pi}\frac{1}{r^3}[2(m_x\sin\theta\cos\phi\, m_y\sin\theta\sin\phi + m_z\cos\theta)]$$

$$B_\theta = \frac{\mu_0}{4\pi}\frac{1}{r^3}[m_x\cos\theta\cos\phi + m_y\cos\theta\sin\phi - m_z\sin\theta]$$

$$B_\phi = \frac{\mu_0}{4\pi}\frac{1}{r^3}[-m_x\sin\phi + m_y\cos\phi]$$

The magnetic force acting on the magnet is calculated by integrating the interaction between the surface magnetization and the magnetic field. This interaction varies across the surface depending on direction and local field strength. The total force is obtained by summing contributions from all surface elements in spherical coordinates.

This result helps explain how the suspended magnet is pulled or pushed depending on its orientation and position.

spherical coordinates

$$r \qquad \theta \qquad \phi \qquad\qquad \mathrm{B} = \mathrm{B_r}\hat{\mathrm{r}} + \mathrm{B_\theta}\hat{\theta} + \mathrm{B_\phi}\hat{\Phi}$$

$$\vec{F}_{mag} = \iint_S R^2\sin\theta\, d\theta d\phi \begin{bmatrix} K_\theta B_\phi - K_\phi B_\theta \\ K_\phi B_r - K_r B_\phi \\ K_r B_\theta - K_\theta B_r \end{bmatrix}$$

The equations describe how the magnet swings on a spherical path, with θ and φ influencing each other. Their coupling reflects the complex angular dynamics of the motion.

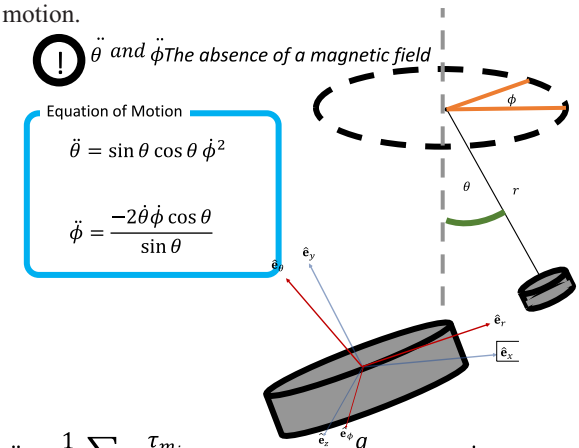

$$\ddot{\theta} = \frac{1}{ml}\sum_i \frac{\tau_{m_i}}{|\mathbf{r}-\mathbf{r_i}|^5}\hat{\mathbf{e}}_\theta.(\mathbf{r}-\mathbf{r_i}) - \frac{g}{l}\sin\theta - \gamma\dot{\theta}$$

$$\ddot{\phi} = \frac{1}{ml\sin\theta}\left[\sum_i \frac{\tau_{m_i}}{|\mathbf{r}-\mathbf{r_i}|^5}\hat{\mathbf{e}}_\phi.(\mathbf{r}-\mathbf{r_i}) - 2\dot{\phi}\dot{\theta}\cos\theta - \gamma\dot{\phi}\right]$$

Gravitational Force:

$$\ddot{\theta}_g = \frac{-g}{l}\sin\theta$$

String Tension Force:

$$\ddot{\theta}_T = \frac{g}{l}\sin(\theta) - \frac{1}{l}\cos(\theta)\dot{\theta}^2\phi$$

$$\ddot{\phi}_T = -2\cot(\theta)\dot{\theta}\dot{\phi}$$

Drag Force:

$$F_{\theta_D} = -mrC_d\frac{\ddot{\theta}}{\dot{\theta}}$$

$$F_{\phi_D} = -mrC_d\sin\frac{\ddot{\phi}}{\dot{\phi}}$$

These expressions calculate the distance between the suspended magnet and the fixed base magnets as a function of the angle θ (Fig. 4).

As the magnet swings, both the vertical and horizontal components change, affecting the magnetic.

$$r_\theta = \sqrt{(l\sin\theta)^2 + h_\theta^2}$$

$$h_\theta = d + l(1-\cos\theta)$$

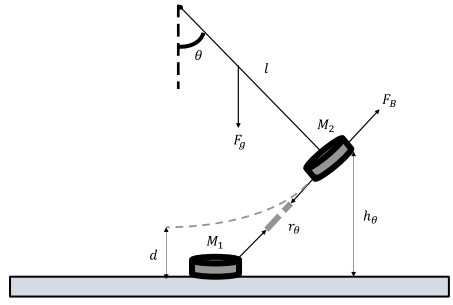

Fig. 4: Applied forces during motion

We considered the moment of inertia of the object as rigid. The sum of the torques are:

$$I_\theta\ddot{\theta} = mgd\theta + \frac{1}{2}c\theta l^2 + \sum_{i=1}^{n}\frac{\psi_i\, l\,\theta}{[(r_i\sin\theta_i\cos\phi_i - l\theta)^2 + (r_i\sin\theta_i\sin\phi)^2 + (r_i\cos\theta_i)^2]^2}$$

Damping Ratio; Torque; $\psi_i = \frac{\mu_0}{4\pi}\frac{m_i}{r_i^3}$

$$I_\phi\ddot{\phi} = mgd\sin\theta\cos\phi - c\dot{\phi} + \sum_{i=1}^{n}\frac{\psi_i\, l\,\theta}{[(r_i\sin\theta_i\cos\phi_i - l\sin\phi)^2 + (r_i\sin\theta_i\sin\phi)^2 + (r_i\cos\theta_i)^2]^2}$$

Gravational Force; Extrnal Torque

$$I_\theta\ddot{\theta}, I_\phi\ddot{\phi} = \sum\tau_i = \tau_{Magnet} + \tau_{Gravity} + \tau_{Damping}$$

Moment of Inertia

$$I_\theta = ml^2$$

$$I_\phi = ml^2\sin^2\theta$$

where;

$m = mass\ of\ magnet$

$l = length\ of\ string$

$c = damping\ coefficient$

$d = distance\ between\ tow\ top\ \&\ down\ magnet$

$\psi_i = The\ influence\ coefficient\ on\ the\ magnetic\ field$

The plotted graph is based on the equations of motion. Azimuth and zenith angles versus time are plotted from the theory. Then using the position of the pendulum, we rewrote the equations and determined the angle formed by the magnet.

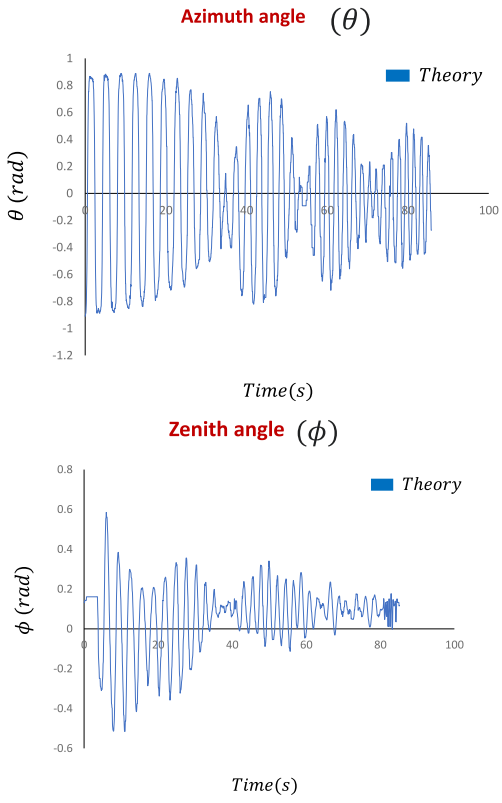

Fig. 5: Two different azimuth and zenith angles versus time

Dynamic Oscillation and the equations to determined the angle formed by the magnet as follows:

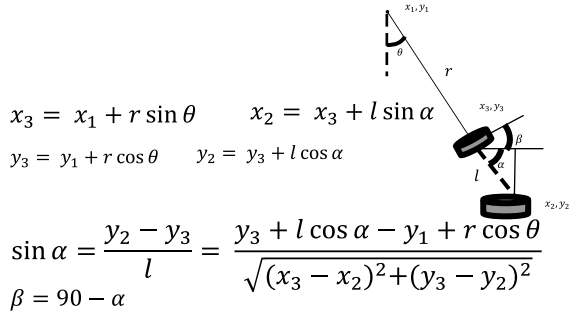

The chart shows the oscillations of the damped system, by the gradual decrease in amplitude over time (Fig. 6).

The stable oscillation frequency despite the decreasing amplitude suggests a constant resistive force and The alignment with the analytical model strengthens the results' validity and the dynamic model's accuracy.

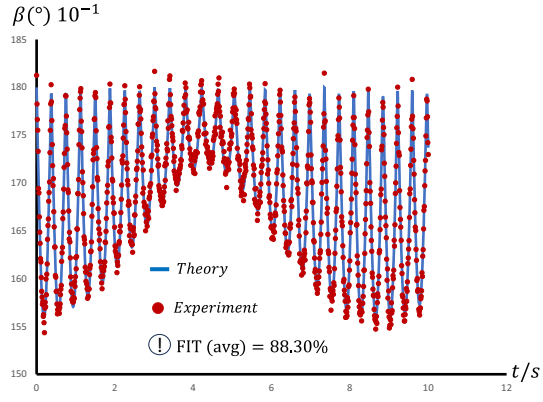

Fig. 6: The oscillation of the damped system

3. Experiment & Results

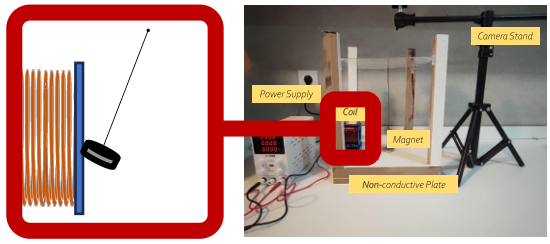

Fig. 7: Experimental setup

A magnet is connected to a coil, and upon deactivating the coil, the magnet is released and coil rapidly moves away . The swinging is seen from top an side views (Fig. 8).

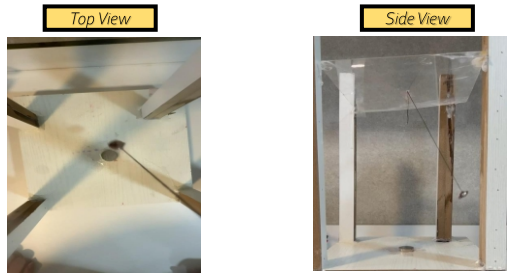

Fig. 8: Swinging of the magnet from top and side views

The experimental setup diagram shows exact places of each items (Fig. 9).

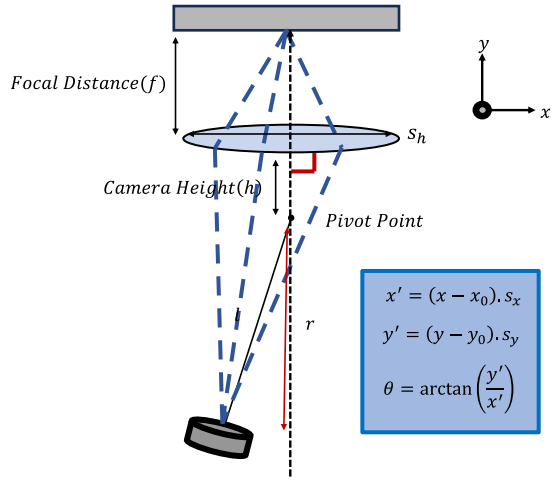

Fig. 9: Schematic of each item

The magnetic field is measured by using a Hall sensor at various angles and distances and damping Coefficient is calculated based on the Logarithmic Decay of Maximum Angular Displacement Over Time".

- Distance of the pendulum from the pivot point in the image plane

$$r = \sqrt{\Delta x^2 + \Delta y^2}$$

- Converting Pixel Coordinates to Real-World Scale

$$d = \frac{r.s_h}{f.p_w}$$

➢ Horizontal Angle of the Pendulum Relative to the Vertical Axis

$$\theta = \arctan\left(\frac{d}{\sqrt{l^2 - d^2}}\right) + \arctan\left(\frac{d}{h}\right)$$

✓ Correcting for Perspective Distortion

$$\theta = \arctan\left(\frac{r.s_h}{f.p_w.\sqrt{l^2 - d^2}}\right) + \arctan\left(\frac{r}{h}\right)$$

The initial experiments are tracked by tracker.

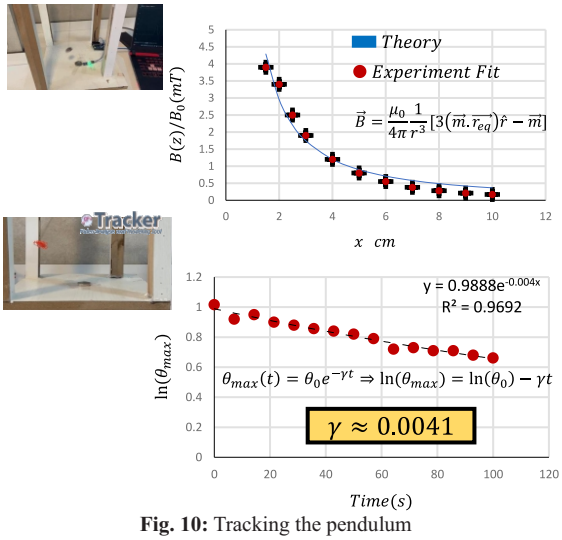

Fig. 10: Tracking the pendulum

The phases are identified based on the amplitude of oscillation (Fig. 11).

Given the low damping coefficient, the system does not come to rest within the observed time interval; however, a gradual decrease in amplitude is evident.

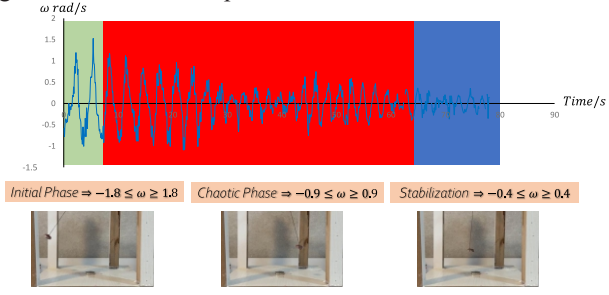

Fig. 11: Different phases

The same effect is clearly observable in the displacement-time graph, where the gradual decay of amplitude due to low damping is evident (Fig. 12).

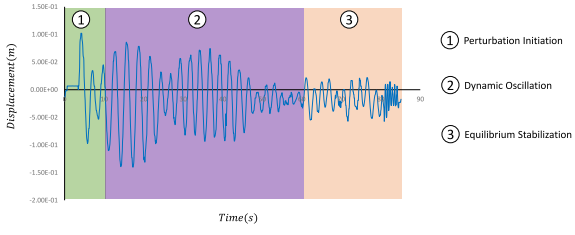

Fig. 12: Displacement

We measured the oscillation period over a defined time interval. However, due to the non-uniformity of the period across different phases, the simple harmonic motion equation is not applicable. Consequently, a modified equation was formulated to account for the time-dependent variation of the period, influenced by the pendulum's dynamics and the magnetic field (Fig. 13).

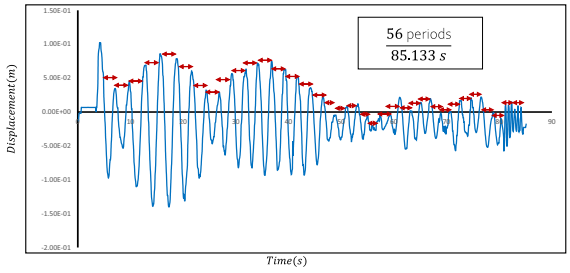

Fig. 13: Displacement vs time

Alternating period:

$$T = 4\int_0^{\theta_{max}} \frac{d\theta}{\sqrt{\frac{2g}{l}(\cos(\theta) - \cos(\theta_{max}) + \frac{2\mathbf{m}B}{Ml^2}[\cos(\theta - \theta_B) - \cos(\theta_{max} - \theta_B)]}}$$

To compare pendulum angle in experiment and theory two angles, azimuth and zenith, are plotted versus time (Fig. 14).

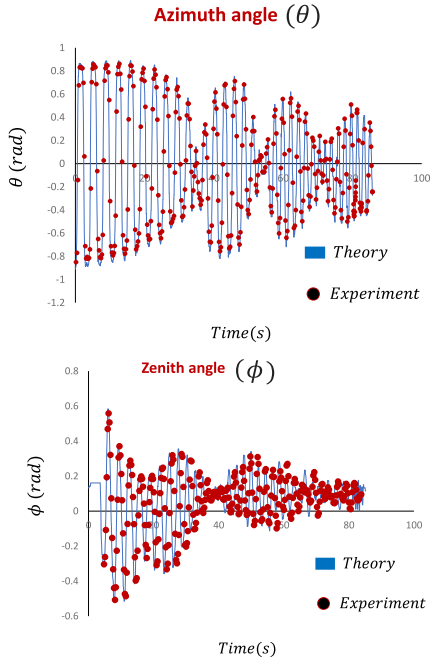

Fig. 14: Comparing azimuth and zenith angles by experiment vs theory

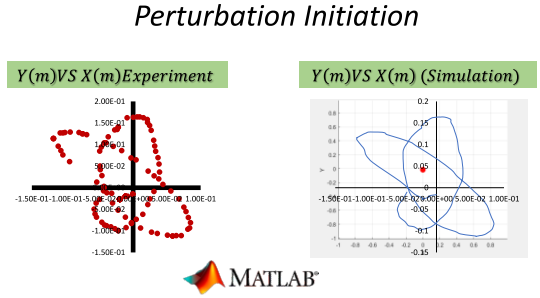

Dynamic Oscillation

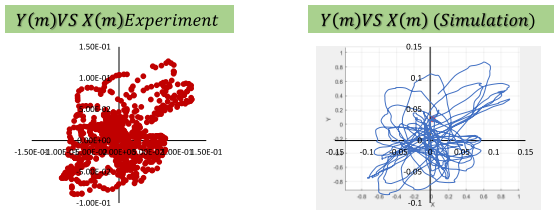

Equilibrium Stabilization

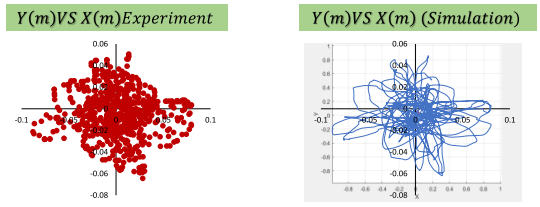

This phenomenon involves the superposition of gravitational and magnetic potential wells. A three-dimensional plot of the combined potential illustrates that gravity forms an upward parabolic profile, whereas the magnetic field introduces a downward parabolic potential centered around the magnet's position (Fig.15).

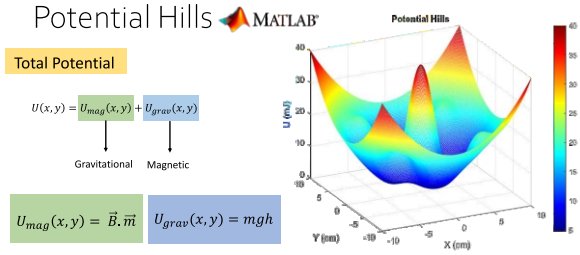

Fig. 15: Potential Hills

When the distance of the magnet increases, the magnetic potential decreases, and the gravitational potential increases. However, when the distance exceeds 8 cm, the magnetic field becomes weak, and the potential becomes 3rd Order (Fig. 16).

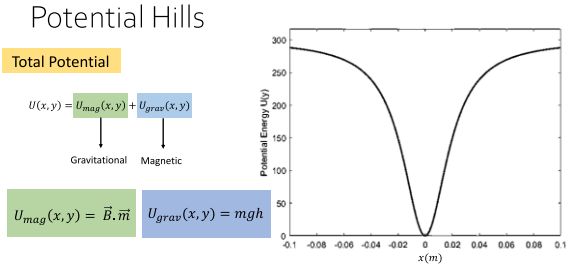

Fig. 16: Potential Hills , 3rd order

4. Parameters Analysis

There are different parameters in this phenomenon which should be considered.

A. Number of Magnets

By increasing the number of magnets, the system reaches a damped state faster and has more damping. However, the pendulum only settles within the magnetic field radius of one of the magnets to reach a stable state, which is why the graph appears this way (Fig. 17).

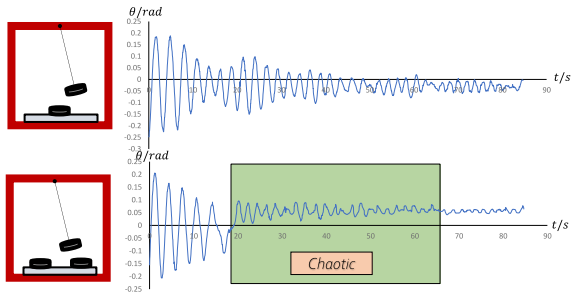

Fig. 17: The effect of number of magnets

B. Distance of the Magnets

In the plot of maximum angular velocity versus distance from the magnet, chaotic motion is observed up to a distance of 3 cm. Beyond this point, the motion becomes non-chaotic. The chaotic behavior is caused by the interference of the magnetic fields of the two magnets, which was confirmed in the experiment using a magnetic field mapping sheet (Fig. 18).

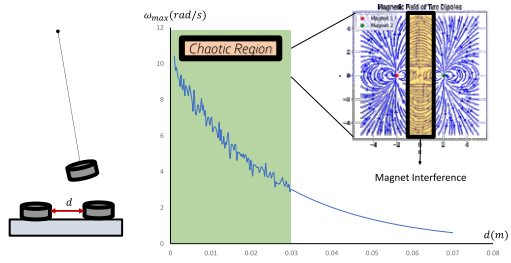

Fig. 18: Distance of the magnets

C. Initial Dropping

According to the theory, the motion follows a logarithmic behavior, which was also observed experimentally. When the data were fitted together, a good agreement between the theoretical prediction and the experimental results was obtained (Fig. 19).

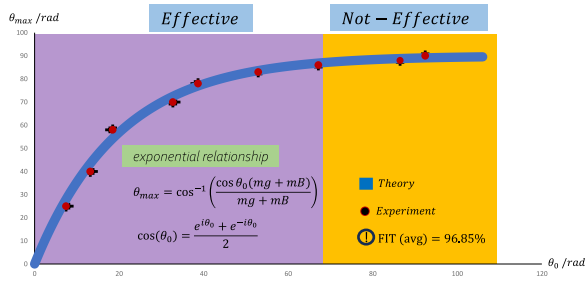

Fig. 19: Initial dropping

D. Distance Between 2 Magnets Down & Top

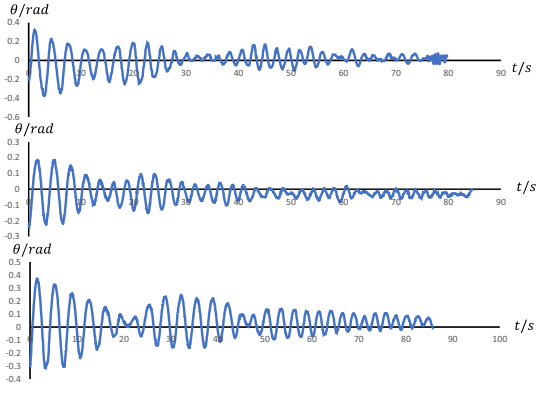

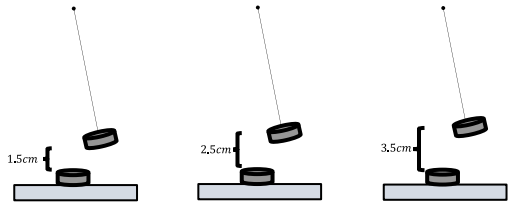

In this section, the first 10 seconds of the graph were plotted, and the amplitudes were compared. The theoretical motion equation was fitted to the experimental data, resulting in a good fit (Fig. 20).

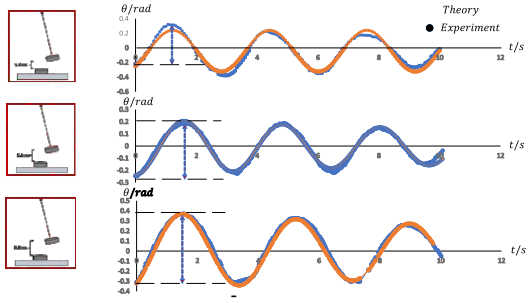

Fig. 20: Angle vs time in different positions of magnets

Frequency is inversely related to the period. Therefore, to plot the theoretical curve, the inverse of the period equation was used (Fig. 21).

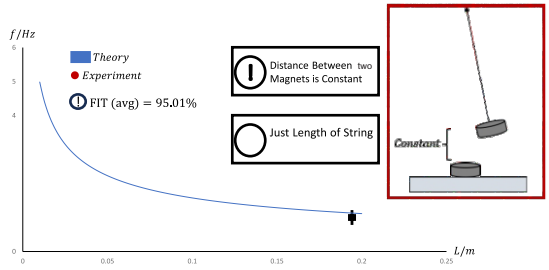

Fig. 21: Frequency Vs the Length of the String

$$f(l) = \left[4\int_0^{\theta_{max}} \frac{d\theta}{\sqrt{\frac{2g}{l}(\cos(\theta)-\cos(\theta_{max}) + \frac{2\mathbf{m}B}{Ml^2}[\cos(\theta-\theta_B)-\cos(\theta_{max}-\theta_B)]}}\right]^{-1}$$

5. Conclusion

- The magnetic field was derived in three-dimensional spherical coordinates
- By the Lorentz force the magnetic force and the term for the matrix of the interaction of magnets were calculated.
- Equation of motion was derived
- Six main parameters were checked and controlled
- Magnetic filed was measured by Hall Effect Sensor
- Damping and drag coefficient were measure
- Based on the fit between theory and experiment, it can be concluded that in the first setup, the equations used exhibit high numerical accuracy, and the tests performed involve a well-designed setup with minimal error.

References

[1] Strogatz, S. H. Nonlinear Dynamics and Chaos: With Applications to Physics, Biology, Chemistry, and Engineering. Westview Press, 2015.

[2] Moon, F. C., & Holmes, P. J. (1979). A magnetoelastic strange attractor. Journal of Sound and Vibration, 65(2), 275–296.

[3] Motter, A. E., Gruiz, M., Károlyi, G., & Tél, T. (2003). Doubly Transient Chaos: Generic Form of Chaos in Autonomous Dissipative Systems. Physical Review Letters, 111, 194101.

[4] Moon, F. C., & Holmes, P. J. (1979). A magnetoelastic strange attractor. Journal of Sound and Vibration, 65(2), 275–296.